Journal of Loss Prevention in the Process Industries 51 (2018) 169–177

Contents lists available at ScienceDirect

Journal of Loss Prevention in the Process Industries

journal homepage: www.elsevier.com/locate/jlp

Configuration factors for ground level fireballs with shadowing

J.A. Vílchez[a], M. Muñoz[a], J.M. Bonilla[b,c], E. Planas[b,*]

[a] TIPs - Trámites, Informes y Proyectos, S.L., Llenguadoc, 17, 08030 Barcelona, Catalonia, Spain
[b] Centre for Technological Risk Studies (CERTEC), Department of Chemical Engineering, Universitat Politècnica de Catalunya·BarcelonaTech, Diagonal, 647, 08028 Barcelona, Catalonia, Spain
[c] Murcia City Council Fire Service & Rescue, Spain

A R T I C L E I N F O

Keywords:
View factor
Sphere
Fireball
Thermal radiation
Aboveground
Firewall

A B S T R A C T

This paper presents new configuration factors for a fireball located at ground level, as radiation emitting source, and a differential receiver, considering the shadow effect of a third finite area that stands between them. The configuration factors were obtained with the combination of a numerical method and a ray-tracing algorithm and are summarized in form of a practical single chart. This work contributes significantly to the knowledge of configuration factors between a sphere and a differential receiver considering the shadow effect because so far, there are no references in existing catalogs in the literature about this specific geometry. Configuration factors serve as inputs for surface-to-surface radiation transport calculations and other like. In chemical engineering, the radiant field produced by a fireball has a strong interest in consequences assessment. Current fireball models do not consider the shadow effect, overestimating vulnerability by thermal radiation and leading to greater safety distances. A case study has been performed to show the interference of a protection wall with respect to the radiation intensity received by a target.

1. Introduction

Diffuse configuration factors play an important role in thermal radiation exchange between surfaces. This parameter is commonly defined as the radiative fraction that leaves a surface '*i*' and directly reaches a surface '*j*'. During the last century, radiation analysis has produced an important set of configuration factors for many engineering applications (Hamilton and Morgan, 1952; Landoni et al., 1962; Dummer and Breckenridge, 1963; Puccinelli, 1973; Hankinson, 1986; Beard et al., 1993; Stasiek, 1998; Bopche and Sridharan, 2010; Bao et al., 2011; Maor and Appelbaum, 2012; Vorre et al., 2015).

In the area of consequences analysis, the thermal radiation field surrounding a fireball is a safety concern of greater relevance. According to The Center for Chemical Process Safety (CCPS), a fireball can be defined as '*the atmospheric burning of a fuel-air cloud in which the energy is mostly emitted in the form of radiant heat. The inner core of the fuel release consists of almost pure fuel whereas the outer layer in which ignition first occurs is a flammable fuel-air mixture. As buoyancy forces of the hot gases begin to dominate, the burning cloud rises and becomes more spherical in shape*' (CCPS, 2010).

The structure and lift dynamics of fireballs have been studied theoretically reporting a typical spherical shape (Hardee and Lee, 1973; Fay and Lewis, 1977; Hasegawa and Sato, 1978; Roberts, 1981; Moorhouse and Pritchard, 1982; IChemE, 1988; Johnson et al., 1990; Prugh, 1991; Shield, 1993; Dorofeev et al., 1995; Maillette and Birk, 1995; Makhviladze et al., 1999a,b; Martinsen and Marx, 1999; Casal et al., 2001; Casal, 2008; CCPS, 2010). But, according to Clay et al. (1988), the shape of a fireball can vary depending on the type of tank failure. In the case of rapid failures, spherical fireballs occur while slower failures tend to produce cylindrical fireballs with high lift-offs. Despite the fact that fireballs do not fit always exactly to the shape of a sphere, the hypothesis of a spherical pattern is in accordance with many of the observations performed in fireballs (Casal, 2008). Therefore, to model and estimate the thermal effects of fireballs in hazard calculations, a spherical shape is usually assumed.

Most of the existing models consider an elevated fireball, with an estimated height of 1.5 times the radius of the fireball (Clay et al., 1988; Shield, 1995; Casal et al., 2001; Van den Bosch and Weterings, 2005), based on the analysis of real accidents and on fireball dynamics. The entraining air stream beside the turbulent increase in volume produces the lift-off of the fireball, evolving towards a spherical shape generated by the buoyancy of the expansion process.

However, fireballs can also be modeled as ground level spherical emitters (Novozhilov, 2003; Stepanov et al., 2011) with its radius just touching the ground throughout its duration (Mannan, 2012). This represents the most conservative case, since the fire is closest to people

* Corresponding author.
E-mail address: eulalia.planas@upc.edu (E. Planas).

https://doi.org/10.1016/j.jlp.2017.12.010
Received 25 July 2017; Received in revised form 31 October 2017; Accepted 13 December 2017
Available online 16 December 2017

and structures, engulfing them. Although hemispherical fireball slightly settled on the ground is quite uncommon, it may occur if the lift-off process of the fireball fails to fully develop for diverse circumstances; such in cases where the initial expansion phase of the vapor cloud is less rapid. In these situations, a larger quantity of liquid will burn at ground level and the general tendency for the cloud to lift-off will be lower. This pattern may occur in accidents where air has difficulties to penetrate into the cloud base, after catastrophic rupture of the container.

Fireballs developed when fuel-air mixtures are ignited in the atmosphere are one of the major hazards in the chemical industry during the storage, processing, and transport of hydrocarbon gases and liquids. Ignition of such a cloud can lead to its explosion accompanied by the generation of blast waves, or to a fire with a significant fraction of the energy of combustion emitted in the form of strong thermal radiation. The massive radiation fluxes from a fireball are capable to trigger secondary ignitions, leading to other fires, loss of life and damage at distances far greater than the size of the burning cloud (Prugh, 1994).

Major accidents, such as those occurred in road and rail transportation (Els Alfacs, Spain, 1978; Lac-Mégantic, Canada, 2013) and gas processing and storage plants (San Juanico, México, 1984; Skikda, Algeria, 2004) are examples of how dangerous the releases of hydrocarbons into the atmosphere can become (Khan and Abbasi, 1999; Abbasi and Abbasi, 2007).

These accidents, among others, revealed the huge hazards of large open hydrocarbon fires that can result in several fatalities. Some work has already been done for the assessment of the heat load exerted by a fireball with respect to a target, i.e. the so-called point source model and solid flame model (Ahlert, 2000). In order to evaluate the thermal radiation reached by a target located at a certain distance from the fireball, the solid flame model is the most commonly used model (Casal, 2008). The solid flame model assumes that the fire is a still, black or grey body, encompassing the entire visible volume of the flames, which diffusively emits thermal radiation from its surface. It requires the determination of the atmospheric transmissivity, of the flame surface emissive power and of the geometric configuration factor between the fireball and the target. Therefore, the shape and size of the fireball and its relative position to the target must be taken into account. When conducting hazard or risk analysis of process vessels or storage tanks that contain flammable liquids or gases, it is important to be able to accurately compute the configuration factor (Makhviladze et al., 1999a,b; Roberts et al., 2000; Novozhilov, 2003; Stepanov et al., 2011).

Current models do not consider the influence of the shade effect exerted by an obstruction like could be the presence of protection walls or the terrain reliefs (hills); thus overestimating the vulnerability by radiation and giving conservative safety distances (i.e. farthest than required).

The main objective of this article is to compute geometric configuration factors between a fireball at ground level and a differential target, considering the shadow effect by a blocking third planar surface. Numerical procedures are briefly presented. This work contributes significantly to the knowledge of configuration factors between a sphere and a differential receiver considering the shadow effect because so far, there are no references to this particular configuration in existing catalogs in the literature. The determination of configuration factors between bodies is of great significance in the calculation of radiative heat exchange, being used as inputs for surface-to-surface radiation transport calculations and other like. In engineering projects related to process, storage or transport of hazardous substances, the radiant field produced by a fireball has a strong interest in consequences assessment. However, very few exact or approximate solutions are available in the literature for the configuration factors when obstruction surfaces must be considered. Analytical solutions for the configuration factors involving spherical body and differential surfaces have been published (Howell et al., 2011). The results are of great interest in various engineering applications, as already indicated above. Nevertheless, these formulations have the following restrictions:

1. In almost all cases, the configuration factor from a sphere to a differential surface is limited to the case where the receiver has full visibility regarding the sphere.
2. In all cases for incomplete visibility, the shielding effects from an intermediate opaque surface are not considered. It is limited to those cases where a surface cannot fully see to the other by virtue of their relative geometrical position.

To the best knowledge of the present authors, the analytical or numerical solutions for the configuration factor from a sphere (i.e. a fireball) to a differential target when a shielding surface is present are not still available in the literature. This article presents, in tabular and graphical form, numerical solutions of the configuration factor for the special case of a fireball located at ground level. Current models do not consider the shadow effect of walls, hills, cliffs or similar structures, overestimating the potential consequences due to the effects of thermal radiation. A case study has been performed to show the interference of a protection wall with respect to the radiation intensity received by a target.

2. Evaluation of configuration factors

The configuration factor between a differential area element and a finite area such as represented in Fig. 1 and equation (1) can be obtained from energy balances (Howell et al., 2011). In the mathematical formulation of the configuration factor the surfaces are considered to be isothermal and diffuse (absorbs and emits diffusively, i.e. the intensity leaving or reaching a surface is independent of direction).

$$F_{dA_2-A_1} = \int_{A_1} \frac{\cos\theta_1 \cdot \cos\theta_2}{\pi \cdot r^2} dA_1 \tag{1}$$

Different methods exist to accurately determine configuration factors (Cohen and Greenberg, 1985; Modest, 2013), which broadly can be classified into analytical, numerical, graphical, experimental and other methods. The graphical and experimental methods were developed when techniques of computation and numerical calculation were not available. Do not allow modeling the shadow effect, require the use of instrumentation and are generally less accurate than the numerical methods. In other methods, we can highlight the radiosity technique and its variants that consist in simulating how light interacts with an environment or scene, calculating the exchange of light between diffuse surfaces. This technique is intended to be used in computer graphics and is not the most suitable for the problem that concerns us, because of the high computational cost of these algorithms. The methods most commonly used in heat transfer calculations are the analytic and numerical methods. Analytic methods such as area and contour integrations are very tedious and, in many cases, it is not possible to get an

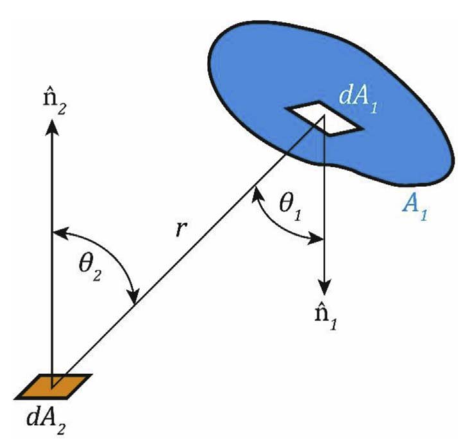

Fig. 1. Scheme for configuration factor definition.

exact analytical solution. This is because it implies the resolution of the canonical equation (1). For this reason, only a few geometrical arrangements have been derived by direct integration. In the particular case of solving the calculation with obstructions, the process may not be further carried out analytically, and numerically means are necessary. Therefore, it becomes imperative the use of numerical computation techniques such as finite elements (Chung and Kim, 1982; Krishnaprakas, 1998), contour integration (Rammohan Rao and Sastri, 1996), Gauss Legendre integration (Mazumder and Ravishankar, 2012) or stochastic Monte Carlo method (Hoff and Janni, 1989) among others. However, it should be mentioned that it does not exist a unique and general method to compute configuration factors for any geometry. It is therefore necessary to use the most appropriate set of techniques that are best suited to each particular problem.

Some authors have applied numerical methods to thermal radiation hazard assessment. Chung and Kim (1982) developed a method combining Gaussian quadrature integration with finite elements, which works very well for irregular geometries. Davis and Bagster (1989, 1990) predicted flame and target geometries for pool and jet fires, calculating configuration factors for both finite and differential target objects, by means of contour integration techniques. Meiers (1998) calculated the radiative impact of flames on three-dimensional surfaces (cylinders) rendering the surfaces according to the radiation they are receiving, taking advantage of the numerical solution suggested by Rein et al. (1970). Other relevant papers are those published by Mudan (1987) and Kay (1994), which provide solutions for geometries usually found in the process industry.

3. Fireball configuration factors

Several authors have contributed to the development of configuration factors between a differential area element and a finite sphere, which can be used to model a fireball event. The simplest case is a differential target perpendicular to the sphere. Crocker and Napier (1988) obtained analytical expressions for the configuration factor of a fireball at ground level in three cases, vertical finite receiver, horizontal differential receiver and vertical differential receiver. Applying it to the particular case at hand, fireball is placed at ground, therefore $H = R = D/2$:

$$F_v = \frac{X_0/R}{\left(\left(\frac{H}{R}\right)^2 + \left(\frac{X_0}{R}\right)^2\right)^{3/2}} = \frac{X_0/R}{\left(1 + \left(\frac{X_0}{R}\right)^2\right)^{3/2}} = \frac{2X_0/D}{\left(1 + 4\left(\frac{X_0}{D}\right)^2\right)^{3/2}} \tag{2}$$

$$F_h = \frac{H/R}{\left(\left(\frac{H}{R}\right)^2 + \left(\frac{X_0}{R}\right)^2\right)^{3/2}} = \frac{1}{\left(1 + \left(\frac{X_0}{R}\right)^2\right)^{3/2}} = \frac{1}{\left(1 + 4\left(\frac{X_0}{D}\right)^2\right)^{3/2}} \tag{3}$$

Derivations for these equations can be found elsewhere (Juul, 1979; Naraghi, 1988; Cabeza-Lainez et al., 2013).

Satyanarayana et al. (1991) drew on the work done by Clay et al. (1988) to predict quantitatively the thermal effects of a fireball. The CCPS (2010) has also provided configuration factors for the case when the differential target is tilted with respect to the sphere. To estimate the thermal radiation from hydrocarbon fireballs, Beyler (2016) also provided these same expressions. This author also studied a case in which the receiver sees the sphere (fireball) partially, providing an analytical expression for the configuration factor. This particular case of incomplete visibility corresponds to the situation in which the receiver's tilt does not allow fully seeing the fireball and does not represent the obstruction caused by a surface.

The maximum value of the configuration factor from a fireball (Fig. 2) is given by equation (4) (Van den Bosch and Weterings, 2005):

$$F_{max} = \left(\frac{R}{d}\right)^2 = \frac{1}{1 + 4\left(\frac{X_0}{D}\right)^2} \tag{4}$$

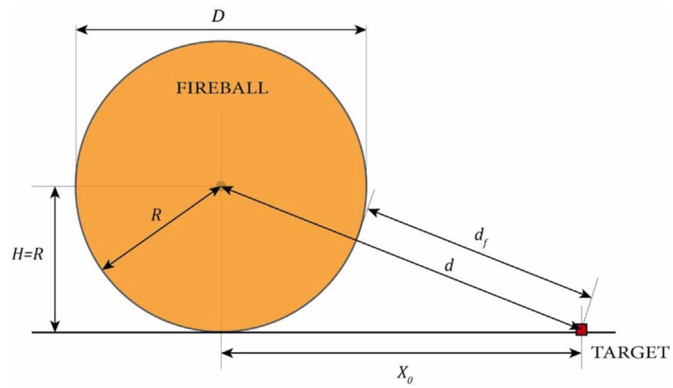

Fig. 2. Scheme of the geometry of a ground level fireball.

It can be demonstrated that equation (4) is equivalent to the square root of the sum of squares of vertical and horizontal configuration factors defined in equations (2) and (3). In this paper, the maximum configuration factor from equation (4) will be used to compare shaded vs unshaded thermal radiation from a fireball.

Additional configuration factors between a sphere and a differential element are available in Howell's catalog of configuration factors (Howell et al., 2011). Recently, Cabeza-Lainez et al. (2013) have developed an analytical expression providing configuration factors between a sphere and a differential element placed at a random position. These factors differ from those obtained by Crocker and Napier (1988) in the relative position of the differential element with respect to the sphere and could be used to determine calculations of fireballs for targets at different positions and orientations.

The only work found in the literature dealing with configuration factors with the presence of a wall is from Papazoglou et al. (2003). It provides a model for estimating heat radiation around pool tank fires in the presence of a protection wall. In this case, the effect of the wall is calculated between a differential target and a cylindrical pool fire. Two positions of the cylinder are considered: aboveground and elevated. The proposed method takes advantage of the configuration factor provided by Raj (1977) and of energy conservation relations instead of numerical calculations.

The literature review revealed that currently, no configuration factors exist to describe the shadow effect induced by a planar surface (wall) and the thermal radiation blockage effect for ground-level fireballs.

The new factors obtained in this survey, previously unpublished in the literature, are presented in a simple graph form for the first time. This paper also provides a versatile tool to radiative consequence analysis as it allows determining the thermal radiation dose for targets at an arbitrary position partially obstructed by a planar wall. On this basis, it will be possible to determine the configuration factor for geometries of practical interest without using numerical calculation techniques.

4. Mathematical model

Fig. 3 shows a representation and general formulation of the system. A sphere of diameter D defines the fireball and is placed on the ground. Its radius R defines, therefore, the height of the sphere center. A differential target is located at a distance X_0. In between, the firewall obstruction is characterized by its elevation, Z_w, and its distance with respect to the sphere's vertical origin, X_w. Nevertheless, an intermediate key variable Z_p is defined, representing the vertical projection of the wall height, from the target to the sphere axis.

Applying Thales' theorem, the relationship between the independent variables X_0, X_w and Z_w can be found:

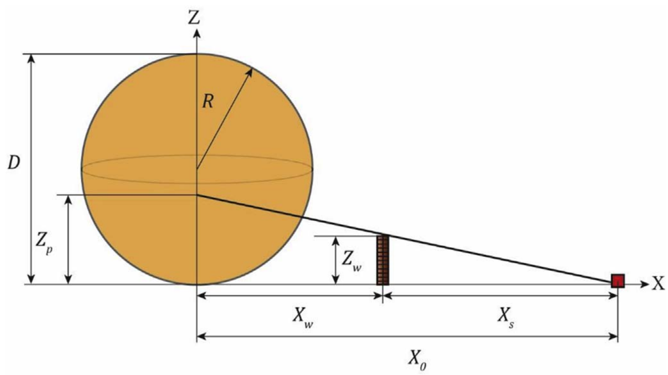

Fig. 3. Scheme of ground level fireball and target with the presence of a wall.

$$Z_p = \frac{Z_w \cdot X_0}{X_0 - X_w} = \frac{Z_w \cdot X_0}{X_s} \tag{5}$$

As it can be inferred from equation (5), Z_p represents a set of different combination of $[X_0,\ X_w,\ Z_w]$ values producing the same shade effect. When Z_w values become very small, the interference induced by the wall is not a controlling effect, and for the limit case of $Z_w = 0$, the maximum configuration factor is determined by the well-known equation (4). On the other hand, when the height of the wall approaches the diameter of the sphere, the configuration factor tends to zero, whatever the value of X_0. Now let's define two new dimensionless variables:

$$Z_d = \frac{Z_p}{D} = \frac{Z_w \cdot X_0}{2 \cdot R \cdot X_s} \tag{6}$$

$$X_d = \frac{X_0}{D} \tag{7}$$

In this manner, four independent variables $(X_0,\ X_w,\ Z_w,\ D)$ can be transformed in only a pair $(Z_d,\ X_d)$, simplifying considerably the mathematical treatment of the problem and allowing to draw the configuration factor solutions in a universal set of charts $F_{max}^{w} = f\,(Z_d,\ X_d)$.

The method used here to determine the configuration factor between a differential element and a sphere is shown in Fig. 4. It is based on the discretization of the sphere in small differential triangles and then performing the numerical integration. The algorithm was developed by Hankinson (1986), to calculate configuration factors between flames and receiving targets for a wide range of geometries involved in large-scale fires. The application of this method to the particular case of a spherical emitter located on the ground leads to the following equation of the configuration factor for each triangular element i:

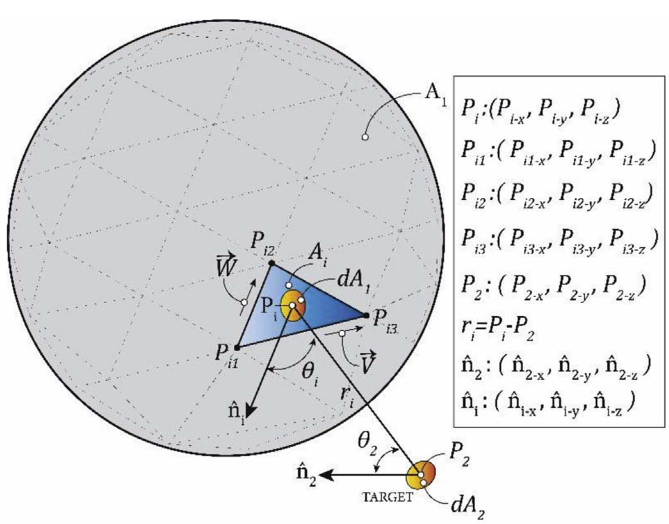

Fig. 4. Triangular finite elements used to represent fireball geometry.

$$F_i = \begin{cases} \frac{\cos\theta_i \cdot \cos\theta_2}{\pi \cdot r_i^2} \cdot A_i, & \forall\ \theta_i \wedge \theta_2 \le 90^\circ \\ 0 & \forall\ \theta_i \wedge \theta_2 > 90^\circ \end{cases} \tag{8}$$

The previous condition allows distinguishing between those elements that are viewed by the receiver (in which case both angles must be less than or equal to 90°) and those which are not. The overall configuration factor is then obtained considering the individual contribution of each element:

$$F_{dA_2-A_1} = \sum_{i=1}^{N} F_i = \sum_{i=1}^{N} \frac{\cos\theta_i \cdot \cos\theta_2}{\pi \cdot r_i^2} \cdot A_i \tag{9}$$

Subsequent mathematical development is based on vector calculus. The accuracy of the method depends on the number of discretization elements of the flame (N_e). More elements imply smaller size of the faces forming the flame, achieving a better accuracy. Another factor to consider is the separation between emitter and receiver. The shorter the distance, the greater should be the number of elements to achieve an acceptable accuracy.

The shadow effect induced by a third surface may be modeled with a ray-tracing technique, combined with the former algorithm. In this case, the algorithm used is the one proposed by Badouel (1990), which is a method easy to implement and highly efficient in determining when a connection line intersects a triangle in space. The application of this method is restricted to convex polygons. Fig. 5 shows the algorithm used to determine the configuration factor for the particular geometry of on-ground fireball obstructed by a convex polygon.

Thus, the application of the algorithm to this particular case consists in tracing precise rays from the points on the center of visible triangles to the target, checking whether there is an intersection between the emitting and obstructing surface. For those cases in which there is an intersection, the configuration factor will be zero. Conversely, if the ray bypasses the obstacle and reaches the target area, the computed configuration factor will be determined from a geometrical relationship based on the numerical method explained so far.

For the system considered, the configuration factor can be subdivided into three sections. A first one, when $Z_d = 0$, there is no obstacle and the result corresponds to the theoretical value provided by equation (4). A second one, when $Z_d > 0$, configuration factor is determined by numerical calculation and it decreases with increasing Z_d and X_d. Finally a third one, when $Z_d = Z_{sd}$ and the configuration factor becomes null. According to Fig. 6, it is possible to derive analytically, using Euclidean geometry, the limit value, Z_{sd}:

$$Z_{sd} = \frac{Z_s}{D} = \frac{1}{1 - \frac{1}{(2X_d)^2}}\ ; \quad \forall\ \ X_d > 1/2 \tag{10}$$

Equation (10) is only valid for X_d values greater than one-half since when it tends to that value; the slope becomes vertical and Z_{sd} grows asymptotically to infinity. For a very remote receiver ($X_d \gg 1/2$), Z_{sd} value tends to unity.

Based on equation (10), for each X_d, it is possible to know the minimum value of Z_d providing a complete blockage of vision between the fireball and the target.

Once, Z_{sd} is known, either the wall height or the separation that is necessary to protect a given target located at a distance X_0 from the fireball can be determined. The wall geometric factor that yields null configuration factor can be defined by:

$$f_w = \left(\frac{Z_w}{X_s}\right)_{F=0} \ge \frac{Z_{sd}}{X_d} \ge \frac{1}{X_d - \frac{1}{4X_d}} \tag{11}$$

Equation (11) has great utility in terms of planning and protection of vulnerable elements in the process industry. A design fireball can be established for each process vessel and therefore, the location and

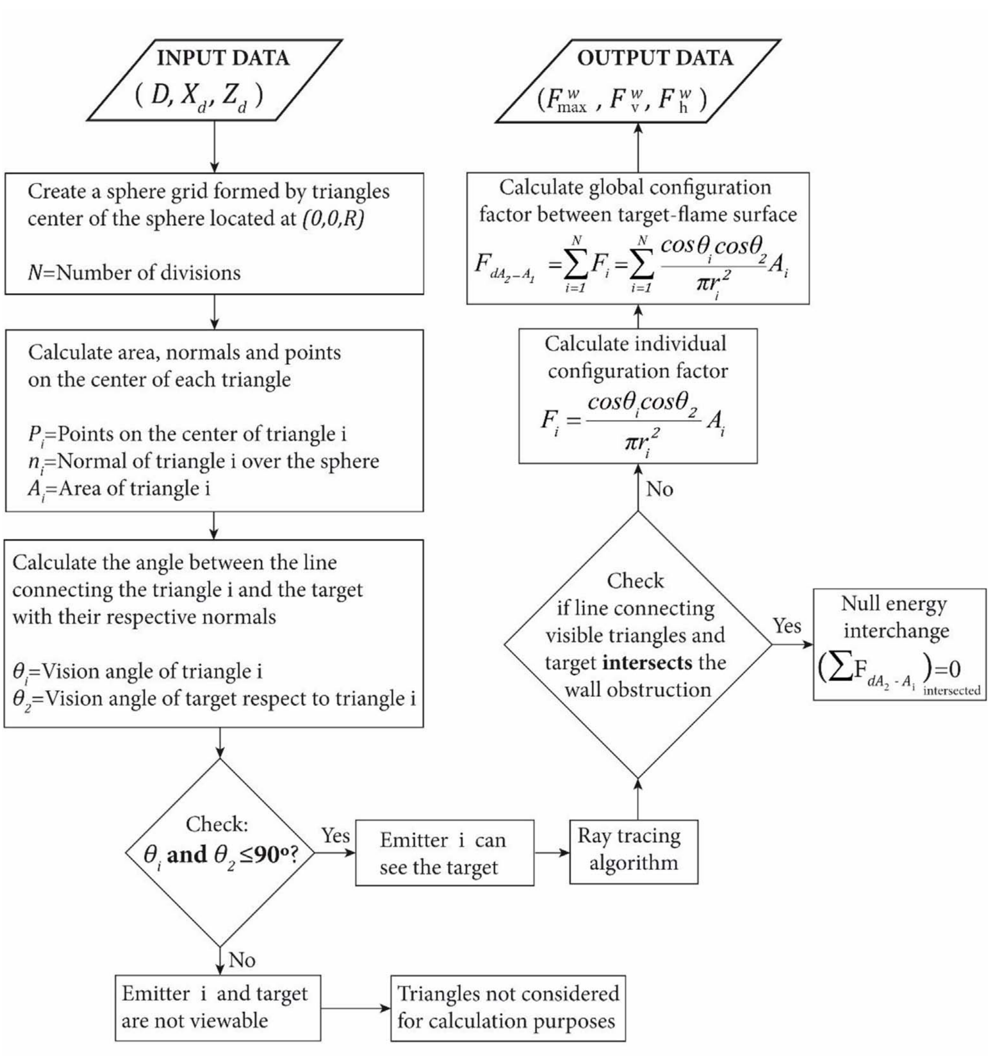

Fig. 5. The algorithm used to calculate the configuration factor between the ground level fireball and a differential target with an obstructing wall.

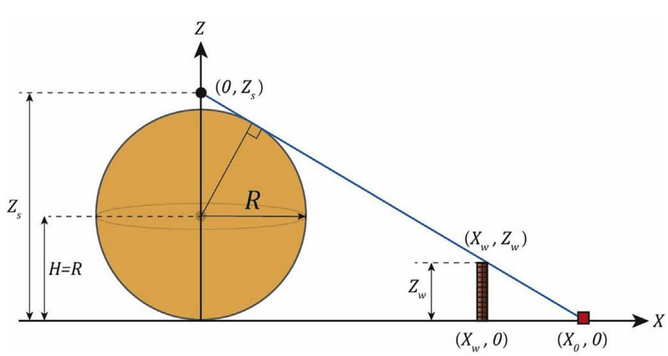

Fig. 6. System geometry configuration that yields a null configuration factor.

settings of the protection firewall can be estimated.

When Z_d is less than the limit value Z_{sd}, a given portion of the fireball surface will be seen by the target.

5. Results and discussion

Different calculations have been performed for the fireball at ground level. Results corresponding to the maximum configuration factor (F^{w}_{max}) are shown in Fig. 7, with a double logarithmic graph for better data representation. Moreover, values are calculated from X_d = 0.55, which corresponds to a receiver located outside the vertical

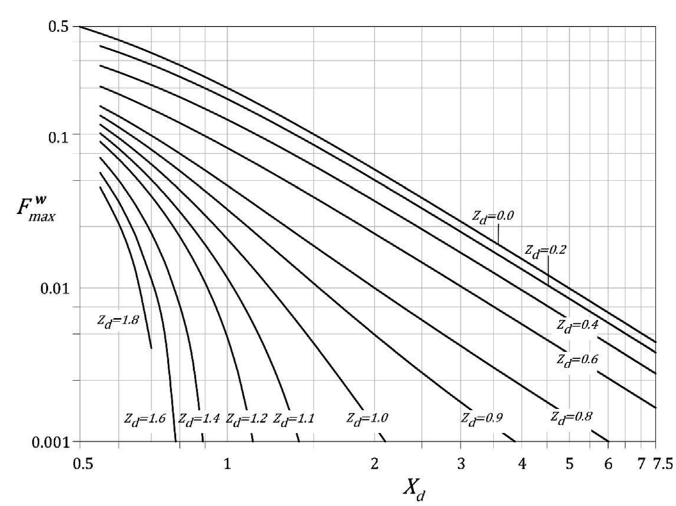

Fig. 7. Ground level fireball configuration factors representation for diverse obstacle configurations (N_e = 2.500).

projection of the fireball. Concerning the upper limit of X_d value, authors like Crawley (1982), Baker et al. (1983) and Birk (1996) consider a minimum distance 4R (X_d = 2) safe enough for LPG fireballs. This value considers emergency responders equipped with personal protective equipment. For the general population, they suggest a distance

Table 1
Relative error provided by the numerical method.

N_e	ε (%)
100	$3.32{\cdot}10^{-2}$
500	$1.32{\cdot}10^{-3}$
1000	$3.31{\cdot}10^{-4}$
2000	$8.25{\cdot}10^{-5}$
3000	$3.67{\cdot}10^{-5}$
4000	$2.06{\cdot}10^{-5}$
5000	$1.82{\cdot}10^{-5}$
6000	$1.26{\cdot}10^{-5}$

between 15 and 30R ($7.5 \le X_d \le 15$), being the value of 30R very conservative, especially for volumes lower than 5 m^3. For calculation purposes, the maximum value of X_d has been set to 7.5.

The system behavior keeps certain likeness to the exponential decay model, although the law is not completely fulfilled and therefore the configuration factor cannot be obtained by multiplying the previous one by a constant coefficient less than 1. The data correlation is nearly linear until $Z_d \approx 0.8$. As Z_d increases from 0.8, the influence of the wall becomes quite important so that the configuration strongly decreases. When the wall height is zero, i.e. no obstruction is present, the configuration factor obtained numerically can be compared with the analytic value provided by equation (4) (see Table 1). Note that even with a relatively small number of triangular elements, the error is always kept below 0.05%.

Tables 2 and 3 provide, respectively, the values of the vertical and horizontal configuration factors obtained using $N_e = 2.500$ elements.

The influence exerted by the wall regarding the configuration factor can be summarized in Fig. 8. The ratio of configuration factor in the presence of a wall with respect to the theoretical value without a wall is illustrated in Fig. 8 for different Z_d values. This graph shows, as expected, the reducing trend of the configuration factor ratio with increasing the height of the wall. Data shown correspond to the mean configuration factor ratio to X_d in the range 0.55–5, with the error bars representing the mean standard deviation. For $Z_d = 0$, the wall height is zero and the configuration factor is calculated by equation (6). For this scenario, there is no reduction and the value is equivalent to the theoretical one, getting 100% value. For instance, if we increase the wall height up to $Z_d = 0.4$, the configuration factor diminishes a 40%. The increase of 0.2 Z_d units represents approximately a decrease of an additional 20% of the factor until Z_d approaches the value 1.0. In this region, the relationship between variables is nearly linear, as can be appreciated in the graph. When $Z_d = 0.9$, the factor is only 10% of the theoretical value, which means an almost total blockage of the target by the fireball. Above $Z_d = 1$, the configuration factor ratio decreases asymptotically to zero.

The above relationship can be fitted to a curve $F_{max}^{w} = F_{max}{\cdot}f(Z_d)$, so that a gross estimation of configuration factor could be determined from the calculation of the theoretical value and solving the projection factor function, for a particular shade effect:

$$f(Z_d) = (a_1 Z_d^6 + a_2 Z_d^5 + a_3 Z_d^4 + a_4 Z_d^3 + a_5 Z_d^2 + a_6 Z_d + a_7) \quad (12)$$

with the following values of the coefficients, a_i:

$a_1 = 0.8052$; $a_2 = -4.1954$; $a_3 = 7.4713$; $a_4 = -4.6899$; $a_5 = 0.3165$; $a_6 = -0.675$; $a_7 = 1.0006$.

$R_{squared} = 0.9998$.

6. Case study

Consider a railway accident of dangerous goods in an urban area that as a result, causes a fire in a 110 m^3 tank car, 85% filled with LPG. After a time, the vessel collapses and a fireball occurs. The content of the vessel just before the explosion was three quarters the initial one, which represents a mass of 34,250 kg. Closest houses are 185 m away from the rail line. This residential area is separated about 10 m from the railroad zone of influence by a solid fence panel 2 m high.

Data: Ambient temperature: 298 K; $HR = 50\,\%$ (partial pressure of water vapor, 1.155 Pa); $H_c = 45{,}000$ kJ/kg.

Solution:

Fireball diameter, its duration, and related parameters can be estimated, according to several correlations collected by Casal et al. (2001):

$$D = 6.14{\cdot}M^{0.325} = 183m$$

$$t = 0.41{\cdot}M^{0.340} = 14.3\,s$$

$$\tau = 2.02(P_w.\ d_f)^{-0.09}$$

Before continue, we must determine the distance between the flame and the target (Fig. 2). Using basic Pythagoras, we get a quadratic equation:

$$d_f^2 + 2Rd_f - X_0^2 = d_f^2 + 183d_f - 34225 = 0$$

Which positive root is $d_f = 114$ m. Thus, atmospheric transmissivity is:

$$\tau = 0.69$$

The emissive power can be determined, assuming $\eta = 0.25$:

$$E_p = \frac{\eta\, M\, H_c}{\pi\, D^2\, t} = \frac{0.25{\cdot}34250{\cdot}45000}{\pi{\cdot}183^2{\cdot}14.3} = 257\,kW{\cdot}m^{-2}$$

Now we get the dimensionless parameters of the system:

$$X_d = \frac{X_0}{D} = \frac{185}{183} \cong 1.0$$

Table 2
Vertical configuration factors F_v^w, for a ground level fireball ($N_e = 2.500$).

Z_d	X_d									
	0.55	0.75	1.0	2.0	3.0	4.0	5.0	6.0	7.0	7.5
0.0	0.3348	0.2560	0.1788	0.0570	0.0266	0.0152	0.0098	0.0069	0.0051	0,0044
0.2	0.2423	0.2008	0.1460	0.0483	0.0227	0.0130	0.0084	0.0059	0.0043	0,0038
0.4	0.1492	0.1336	0.1011	0.0348	0.0165	0.0095	0.0061	0.0043	0.0032	0,0028
0.6	0.0907	0.0823	0.0619	0.0209	0.0098	0.0056	0.0036	0.0026	0.0019	0,0016
0.8	0.0570	0.0482	0.0329	0.0090	0.0040	0.0022	0.0014	0.0010	0.0007	0,0006
0.9	0.0459	0.0363	0.0222	0.0044	0.0017	0.0009	0.0005	0.0004	0.0003	0,0002
1.0	0.0373	0.0269	0.0138	0.0011	0.0001	4.6E-5	1.5-E5	6.5E-6	3.0E-6	2.1E-6
1.1	0.0307	0.0195	0.0074		Null					
1.2	0.0254	0.0138	0.0029							
1.4	0.0179	0.0060								
1.6	0.0129	0.0017								
1.8	0.0095									

Table 3
Horizontal configuration factors, F_h^w for a ground level fireball ($N_e = 2.500$).

Z_d	X_d									
	0.55	0.75	1.0	2.0	3.0	4.0	5.0	6.0	7.0	7.5
0.0	0.3043	0.1706	0.0894	0.0142	0.0044	0.0019	0.0009	0.0006	0.0004	0.0003
0.2	0.2855	0.1622	0.0856	0.0137	0.0042	0.0018	0.0009	0.0006	0.0003	0.0003
0.4	0.2357	0.1355	0.0721	0.0117	0.0036	0.0015	0.0008	0.0005	0.0003	0.0002
0.6	0.1835	0.1017	0.0527	0.0082	0.0025	0.0010	0.0005	0.0003	2.1E-4	1.7E-4
0.8	0.1412	0.0703	0.0326	0.0041	0.0011	0.0004	0.0002	1.5E-4	9.2E-5	7.5E-5
0.9	0.1241	0.0567	0.0235	0.0021	0.0005	0.0002	0.0001	6.0E-5	3.7E-5	3.0E-5
1.0	0.1093	0.0449	0.0155	0.0005	6.1E-5	1.1E-5	3.1E-6	1.1E-6	4.4E-7	2.9E-7
1.1	0.0966	0.0346	0.0088							
1.2	0.0857	0.0258	0.0037		Null					
1.4	0.0680	0.0125								
1.6	0.0545	0.0039								
1.8	0.0441									

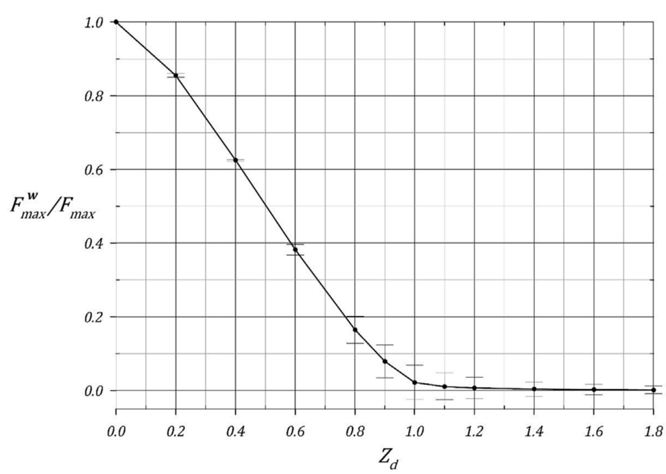

Fig. 8. Ratio between maximum configuration factor with and without wall as a function of Z_d.(Standard deviation error bars)

$$Z_d = \frac{X_0 Z_w}{X_s D} = \frac{185\cdot 2}{10\cdot 183} \cong 0.2$$

Then, from Fig. 7, the maximum value of the configuration factor can be obtained:

$$F^w_{max}(X_d,\ Z_d) = F^w_{max}(1.0,\ 0.2) = 0.169$$

The radiation intensity will be:

$$I_w = \tau\cdot F^w_{max}\cdot E_p = 0.69\cdot 0.169\cdot 257 = 30\ kW\cdot m^{-2}$$

The fatality rate can be estimated using the Probit function proposed by Eisenberg et al. (1975):

$$\text{Y}= -14.9 + 2.56\cdot\ln\left(I_w^{\frac{4}{3}}t\right) = -14.9 + 18.4 = 3.5$$

Which represents a 7% of the population affected.

A fireball is a transient event, and its impact should be assessed in terms of thermal dose rather than thermal intensity. The level of intensity, duration of exposure and percentage of exposed bare skin result in a received thermal radiation dose (TDU), which can be calculated and used to estimate these effects by the following equation:

$$\text{D}_{\text{tw}} = I_w^{\frac{4}{3}}t = 30^{\frac{4}{3}}\cdot 14.3 = 1333\ (kW\cdot m^{-2})^{\frac{4}{3}}s$$

Eisenberg et al. (1975) established the value of 1000 *TDU* as a dangerous dose, which would give rise to a small probability of fatality for an average population, with second-degree burns (1% Fatality).

We can also estimate the wall height that provides a null configuration factor:

$$(Z_w)_{F=0} = \frac{Z_{sd}X_s}{2X_d} = \frac{X_s}{2X_d - \frac{1}{2X_d}} = \frac{10}{\frac{3}{2}} = 6.66\ m$$

As a result, the engineered protection barriers in process plants and urban areas are suitable as an effective system to reduce the levels of thermal radiation for a given objective.

7. Conclusions

This paper provides a new and important contribution to configuration factor's literature, as up to date a factor for fireballs (spheres) with shadowing has not yet been published. The algorithm used provides results with a great accuracy for a small number of divisions and short execution time.

The geometric configuration for which the factor is null has been analytically determined. With the increasing height of the wall, the relative sight between the fireball and target decreases, until the receiver is eclipsed and the configuration factor becomes zero. This condition could be used to protect areas vulnerable to thermal radiation, for different hypotheses of fireball design.

In terms of methodological utility, this paper provides a reproducible strategy for similar scenarios. Opens new research lines in three different ways: configuration factors of spheres with blocking surfaces, which can be exploited for the development of new factors; modeling thermal radiation of fireballs with the presence of barriers and design of protective barriers in the vicinity of the process industries. Specifically, it can be used to get the optimal location of the storage tanks and the design of engineered barriers for the protection of persons and property near the industries that store or transport flammable substances.

As a practical tool it can solve a common problem in risk analysis, allowing a more realistic engineering modeling, providing knowledge and tools about an effect not considered so far. Through diagrams reading, configuration factor is obtained immediately without performing the numerical calculation, an issue that is very useful for analysts in technological risks.

Acknowledgements

The authors are grateful to the Spanish Ministry of Economy and Competitiveness (project CTM2014-57448-R, funded with FEDER funds).

Appendix A. Supplementary data

Supplementary data related to this article can be found at http://dx.doi.org/10.1016/j.jlp.2017.12.010.

Nomenclature

a_i	Coefficients of curve fitting, -
A_i	Area of element 'i', m^2
d	Distance between the center of fireball and the target, m
d_f	Distance between the flame and the target, m
dA_2	Differential area of surface 2, m^2
D	Fireball diameter, m
D_t	Thermal dose, $kW^{4/3}\,s\,m^{-8/3}$
D_{tw}	Thermal dose with the presence of the wall, $kW^{4/3}\,s\,m^{-8/3}$
E_p	Emissive power, $kW{\cdot}m^{-2}$
ε	Relative error, %
η	Fraction mass involved in the explosion, -
F	Configuration factor,-
F_i	Configuration factor of element "i",-
F_v	Configuration factor for a target-oriented vertically, (theoretical), —
F_h	Configuration factor for a target-oriented horizontally, (theoretical), —
F_v^w	Configuration factor for a target-oriented vertically considering the presence of the wall (numerical),-
F_h^w	Configuration factor for a target-oriented horizontally considering the presence of the wall (numerical),-
$F_{dA_1-A_2}$	Configuration factor between differential area element and finite area, -
F_{max}	Maximum value of configuration factor between fireball and target (theoretical), -
F_{max}^w	Maximum value of configuration factor between fireball and target considering the presence of the wall (numerical),-
H_c	Heat of combustion, $kJ{\cdot}kg^{-1}$
HR	Relative humidity, %
I	Radiation intensity, $kW{\cdot}m^{-2}$
I_w	Radiation intensity with the presence of the wall, $kW{\cdot}m^{-2}$
θ_1, θ_2	Vision angles between the surface normals and the line of length r between them, radians
θ_i	Vision angle of element 'i'
M	Fireball mass, kg
N_e	Number of elements of the flame, -
n_i	Normal vector of triangle 'i', -
n_2	Normal vector of target, -
P_i	Cartesian coordinates of triangle barycenter, m
P_w	Partial pressure of water vapor, Pa
r	Distance between differential and finite area elements, m.
r_i	Distance between differential element 'i' and target, m.
R	Fireball radius, m
$R_{squared}$	Coefficient of determination, -
t	Fireball duration, s
TDU	Thermal dose unit, $kW^{4/3}\,s\,m^{-8/3}$
τ	Atmospheric transmissivity, -
$\vec{v}$, $\vec{w}$	Vectors defining two edges of the triangle, m
X_0	Ground distance between the center of fireball and the target, m
X_d	Target separation factor, -
X_w	Distance at which wall is placed, m
X_s	Distance between the target and the wall, m
Z_d	Sphere projection factor, -
Z_p	Height at which the projection line outgoing the target and tangent to wall intersects the sphere vertical axis, m
Z_s	Locus height (relative to the ground) that provides complete blockage, m
Z_{sd}	Locus of sphere projection factor, -
Z_w	Wall height, m

References

Abbasi, T., Abbasi, S.A., 2007. The boiling liquid expanding vapour explosion (BLEVE): mechanism, consequence assessment, management. J. Hazard Mater. 141, 489–519. http://dx.doi.org/10.1016/j.jhazmat.2006.09.056.

Ahlert, R.C., 2000. Guidelines for Consequence Analysis of Chemical Releases. Center for Chemical Process Safety, American Institute of Chemical Engineers (AIChE)http://dx.doi.org/10.1002/ep.670190304. ISBN: 0-8169-0786-2.

Badouel, D., 1990. An Efficient Ray-polygon Intersection. Graphics Gems. Academic Press Professional.

Baker, W.E., Cox, P.A., Westine, P.S., Kulesz, J.J., Strehlow, R.A., 1983. Explosion Hazards and Evaluation. Chapter 7. Thermal Radiation Effects. Elsevierhttp://dx.doi.org/10.1016/B978-0-444-42094-7.50015-X. ISBN: 978-0-444-42094-7.

Bao, C., Cai, N., Croiset, E., 2011. An analytical model of view factors for radiation heat transfer in planar and tubular solid oxide fuel cells. J. Power Sources 196, 3223–3232. http://dx.doi.org/10.1016/j.jpowsour.2010.11.128.

Beard, A., Drysdale, D., Holborn, P., Bishop, S., 1993. Configuration factor for radiation in a tunnel or partial cylinder. Fire Technol. 29, 281–288. http://dx.doi.org/10.1007/BF01152111.

Beyler, C.L., 2016. SFPE Handbook of Fire Protection Engineering, Chapter 66. Fire Hazard Calculations for Large, Open Hydrocarbon Fires. Springer New Yorkhttp://dx.doi.org/10.1007/978-1-4939-2565-0. ISBN: 978-1-4939-2564-3.

Birk, A.M., 1996. Hazards from propane BLEVEs: an update and proposal for emergency responders. J. Loss Prev. Process. Ind. 9, 173–181. http://dx.doi.org/10.1016/0950-4230(95)00046-1.

Bopche, S.B., Sridharan, A., 2010. Analytical expressions for configuration factor between cylindrical surfaces in rod bundle geometry. Nucl. Eng. Des. 240, 3020–3036. http://dx.doi.org/10.1016/j.nucengdes.2010.05.011.

Cabeza-Lainez, J.M., Pulido-Arcas, J.A., Castilla, M.-V., 2013. New configuration factor between a circle, a sphere and a differential area at random positions. J. Quant. Spectrosc. Radiat. Transf. 129, 272–276. http://dx.doi.org/10.1016/j.jqsrt.2013.06.027.

Casal, J., 2008. Evaluation of the Effects and Consequences of Major Accidents in Industrial Plants. Industrial Safety Series, vol. 8 Elsevierhttp://dx.doi.org/10.1016/S0921-9110(08)80003-1. ISBN: 978-0-444-53081-3.

Casal, J., Arnaldos, J., Montiel, H., 2001. Handbook of Hazardous Materials Spills Technology. Chapter 22, Modeling and Understanding Bleves. McGraw-Hill Professional ISBN: 978–0071351713.

CCPS, 2010. Guidelines for Vapor Cloud Explosion, Pressure Vessel Burst, BLEVE and Flash Fire Hazards, second ed. Wiley978-0-470-25147-8.

Chung, T.J., Kim, J.Y., 1982. Radiation view factors by finite elements. ASME, Transactions. J. Heat Tran. 104, 792–795. http://dx.doi.org/10.1115/1.3245203.

Clay, G.A., Fitzpatrick, R.D., Hurst, N.W., Carter, D.A., Crossthwaite, P.J., 1988. Risk assessment for installations where liquefied petroleum gas (LPG) is stored in bulk vessels above ground. J. Hazard Mater. 20, 357–374. http://dx.doi.org/10.1016/0304-3894(88)87022-5.

Cohen, M.F., Greenberg, D.P., 1985. The hemi-cube: a radiosity solution for complex environments. In: Proceedings of the 12th Annual Conference on Computer Graphics and Interactive Techniques, vol. 19. pp. 31–40. http://dx.doi.org/10.1145/325334.325171.

Crawley, F.K., 1982. The effects of the ignition of a major fuel spillage, assessment of major hazards. In: IChemE Symposium Series No. 71, pp. 125–145.

Crocker, W., Napier, D., 1988. Assessment of mathematical models for fire and explosion hazards of liquefied petroleum gases. J. Hazard Mater. 20, 109–135. http://dx.doi.org/10.1016/0304-3894(88)87009-2.

Davis, B.C., Bagster, D.F., 1989. The computation of view factors of fire models: 1. Differential targets. J. Loss Prev. Process. Ind. 2, 224–234. http://dx.doi.org/10.1016/0950-4230(89)80037-3.

Davis, B.C., Bagster, D.F., 1990. The computation of view factors of fire models: 2. Finite targets. J. Loss Prev. Process. Ind. 3, 327–329. http://dx.doi.org/10.1016/0950-4230(90)80027-8.

Dorofeev, S.B., Sidorov, V.P., Efimenko, A.A., Kochurko, A.S., Kuznetsov, M.S., Chaivanov, B.B., Matsukov, D.I., Pereverzev, A.K., Avenyan, V.A., 1995. Fireballs from deflagration and detonation of heterogeneous fuel-rich clouds. Fire Saf. J. 25, 4323–4336. http://dx.doi.org/10.1016/0379-7112(96)00008-2.

Dummer, R.S., Breckenridge, W.T., 1963. Radiation Configuration Factors Catalog. General Dynamics Corporation. Astronautics Division Report, ERR-AN-244. .

Eisenberg, N.A., Lynch, C.J., Breeding, R.J., 1975. Vulnerability Model: a Simulation System for Assessing Damage Resulting from Marine Spills (VM1). ADA015245, US Coast Guard, National Technical Information Service Report No. CG-D-137-75. .

Fay, J.A., Lewis, D.H., 1977. Unsteady burning of unconfined fuel vapour clouds. In: 16th Symposium (International) on Combustion, vol. 16. pp. 1397–1405. http://dx.doi.org/10.1016/S0082-0784(77)80424-4.

Hamilton, D.C., Morgan, W.R., 1952. Radiant-interchange configuration factors. National advisory committee for aeronautics. Technical Note 2836, 1–110.

Hankinson, G., 1986. A method for calculating the configuration factor between a flame and a receiving target for a wide range of flame geometries relevant to large-scale fires. Fire Safety Science. In: Proceedings of the First International Symposium, pp. 197–206. http://dx.doi.org/10.3801/IAFSS.FSS.1-197.

Hardee, H.C., Lee, D.O., 1973. Thermal hazard from propane fireballs. Transport. Plann. Technol. 2, 121–128. http://dx.doi.org/10.1080/03081067308717067.

Hasegawa, K., Sato, K., 1978. Experimental investigation of the unconfined vapor cloud explosions and hydrocarbons. Technical Memos of Fire Research Institute of Japan 12, 3–9.

Hoff, S.J., Janni, K.A., 1989. Monte Carlo technique for the determination of thermal radiation shape factors. Trans. Am. Soc. Agric. Eng. 32, 1023–1028. http://dx.doi.org/10.13031/2013.31108.

Howell, J.R., Siegel, R., Pinar Mengüç, M., 2011. Thermal Radiation Heat Transfer, fifth ed. CRC Press, Taylor & Francis, pp. 153–161 ISBN: 9781439866689 M.

The Institution of Chemical Engineers, 1988. Calculation of the intensity of thermal radiation from large fires. Loss Prev. Bull.(082).
Johnson, D.M., Pritchard, M.J., Wickens, M.J., 1990. Large Scale Catastrophic Releases of Flammable Liquids. Commission of the European Communities Report, Contract EV4T.0014.UK(H).
Juul, N.H., 1979. Diffuse radiation view factors from differential plane sources to spheres. J. Heat Tran. 101, 558–560. http://dx.doi.org/10.1115/1.3451029.
Kay, D., 1994. Thermal Radiation Heat Transfer from Flames to Receiving Targets. Report AEA/CSHSE R1006/R for the Health and Safety Executive, UK.
Khan, F.I., Abbasi, S.A., 1999. Major accidents in process industries and an analysis of causes and consequences. J. Loss Prev. Process. Ind. 12, 361–378. http://dx.doi.org/10.1016/S0950-4230(98)00062-X.
Krishnaprakas, C.K., 1998. View-factor evaluation by quadrature over triangles. J. Thermophys. Heat Tran. 12, 118–120. http://dx.doi.org/10.2514/2.6313.
Landoni, J., Sabet, M., Chung, B., 1962. View Factors for Heat Radiation HTGR Core Configuration. U.S. Atomic Energy Commission, pp. 1–24. http://dx.doi.org/10.2172/4736222. Research Report, Project 32.820.
Maillette, J., Birk, A.M., 1995. Effects of tank failure mode and lading properties on propane fireball geometry and fire hazard. In: AIChE International Conference and Workshop on Modeling and Mitigating the Consequences of Hazardous Materials, pp. 721–735.
Makhviladze, G.M., Roberts, J.P., Yakush, S.E., 1999a. Fireball during combustion of hydrocarbon fuel releases. I. Structure and lift dynamics. Combust., Explos. Shock Waves 35, 219–229. http://dx.doi.org/10.1007/BF02674442.
Makhviladze, G.M., Roberts, J.P., Yakush, S.E., 1999b. Fireball during combustion of hydrocarbon fuels releases II. Thermal radiation. Combust., Explos. Shock Waves 35, 359–369. http://dx.doi.org/10.1007/BF02674465.
Mannan, S., 2012. Lees' Loss Prevention in the Process Industries (Chapter 16): Fire. fourth ed. Butterworth-Heinemann, Oxford ISBN:9780123971890 doi:10.1016/B978-0-12-397189-0.00016-1.
Maor, T., Appelbaum, J., 2012. View factors of photovoltaic collector systems. Sol. Energy 86, 1701–1708. http://dx.doi.org/10.1016/j.solener.2012.03.017.
Martinsen, W.E., Marx, J.D., 1999. An improved model for the prediction of radiant heat from fireballs. In: International Conference and Workshop on Modelling the Consequences of Accidental Releases of Hazardous Materials, CCPS. California, San Francisco, pp. 605–621 September 28 – October 1.
Mazumder, S., Ravishankar, M., 2012. General procedure for calculation of diffuse view factors between arbitrary planar polygons. Int. J. Heat Mass Tran. 55, 7330–7335. http://dx.doi.org/10.1016/j.ijheatmasstransfer.2012.07.066.
Meiers, S.J., 1998. Calculating the radiative impact of flames on three dimensional surfaces. In: 17th International Conference on Offshore Mechanics and Arctic Engineering, OMAE98–1442. ASME.
Modest, M.F., 2013. Radiative Heat Transfer (Chapter 4) View Factors. third ed. Academic Presshttp://dx.doi.org/10.1016/B978-0-12-386944-9.50004-2. ISBN: 978-0-12-386944-9.
Moorhouse, J., Pritchard, M.J., 1982. Thermal radiation hazards from large pool fires and fireballs. A literature review. In: The Institution of Chemical Engineers Symposium Series, vol. 71. pp. 397–428.
Mudan, K., 1987. Geometric view factors for thermal radiation hazard assessment. Fire Saf. J. 12, 89–96. http://dx.doi.org/10.1016/0379-7112(87)90024-5.
Naraghi, M.H., 1988. Radiative view factors from spherical segments to planar surfaces. J. Thermophys. Heat Tran. 2, 373–375. http://dx.doi.org/10.2514/3.56226.
Novozhilov, V., 2003. Some aspects of the mathematical modeling of fireballs. Proc. Inst. Mech. Eng., Part E: J. Process Mech. Eng. 217, 103–121. http://dx.doi.org/10.1243/095440803766612775.
Papazoglou, I.A., Aneziris, O.N., Bonanos, G., 2003. Effect of a concrete wall in the limitation of thermal radiation resulting from large industrial fires. In: Proceedings of European Safety and Reliability Conference, vol. 2. Swets & Zeitlinger, pp. 1205–1210.
Prugh, R.W., 1991. Quantitative evaluation of bleve hazards. J. Fire Protect. Eng. 3, 9–24. http://dx.doi.org/10.1177/104239159100300102.
Prugh, R.W., 1994. Quantitative evaluation of fireball hazards. Process Saf. Prog. 13, 83–91. http://dx.doi.org/10.1002/prs.680130211. v13:2/issuetoc" > .
Puccinelli, E.F., 1973. View Factor Computer Program User's Manual. Goddard Space Flight Center. NASA Technical Report, TM-X-70538, X-324-73-272. pp. 1–116.
Raj, P.K., 1977. Calculation of thermal radiation hazards from LNG fires, a review of the state of the art. In: American Gas Association. Transmission Conference, Paper No 2, Session 18, pp. 135–148.
Rammohan Rao, V., Sastri, V., 1996. Efficient evaluation of diffuse view factors for radiation. Int. J. Heat Mass Tran. 39, 1281–1286. http://dx.doi.org/10.1016/0017-9310(95)00203-0.
Rein, R.G., Sliepcevich, C.M., Welker, J.R., 1970. Radiation view factors for tilted cylinders. J. Fire Flammabil. 1, 140–153.
Roberts, A.F., 1981. Thermal radiation hazards from releases of LPG from pressurized storage. Fire Saf. J. 4, 197–212. http://dx.doi.org/10.1016/0379-7112(81)90018-7.
Roberts, T., Gosse, A., Hawksworth, S., 2000. Thermal radiation from fireballs on failure of liquefied petroleum gas storage vessels. Process Saf. Environ. Protect. 78, 184–192. http://dx.doi.org/10.1205/095758200530628.
Satyanarayana, K., Borah, M., Rao, P.G., 1991. Prediction of thermal hazards from fireballs. J. Loss Prev. Process. Ind. 4, 344–347. http://dx.doi.org/10.1016/0950-4230(91)80048-Y.
Shield, S.R., 1993. A model to predict radiant heat and blast hazards from LPG BLEVES. In: AIChE 29th National Heat Transfer Conference, pp. 139–149.
Shield, S.R., 1995. The modelling of BLEVE fireball transients. In: Proceedings of 2nd European Conference on Major Hazards on and Off-shore, Manchester. IChemE Symposium Series, vol. 139. pp. 227–236.
Stasiek, J.A., 1998. Application of the transfer configuration factors in radiation heat transfer. Int. J. Heat Mass Tran. 41, 2893–2907. http://dx.doi.org/10.1016/S0017-9310(98)00024-6.
Stepanov, K.L., Stanchits, L.K., Stankevich, Y.A., 2011. Modeling of explosion thermal radiation. J. Eng. Phys. Thermophys. 84, 179–206. http://dx.doi.org/10.1007/s10891-011-0462-3.
The Center for Chemical Process Safety (CCPS) of the American Institute of Chemical Engineers (AIChE). Process Safety Glossary (available at: http://www.aiche.org/ccps/resources/glossary).
Van den Bosch, C.J.H., Weterings, R.A.P.M., 2005. Methods for the Calculation of Physical Effects-due to Releases of Hazardous Materials (Liquids and Gases), 'Yellow Book', the Committee for the Prevention of Disasters by Hazardous Materials, Director-general for Social Affairs and Employment. (The Hague).
Vorre, M.H., Jensen, R.L., Le Dréau, J., 2015. Radiation exchange between persons and surfaces for building energy simulations. Energy Build. 101, 110–121. http://dx.doi.org/10.1016/j.enbuild.2015.05.005.